

**Adsorbate-mediated step transformations and terrace rearrangement of Si(100)-(2×1)**R. E. Butera,<sup>1</sup> Yuji Suwa,<sup>2</sup> Tomihiro Hashizume,<sup>2</sup> and J. H. Weaver<sup>1</sup><sup>1</sup>*Department of Materials Science and Engineering, University of Illinois at Urbana-Champaign, Urbana, Illinois 61801, USA*<sup>2</sup>*Advanced Research Laboratory, Hitachi Ltd., Kokubunji, Tokyo 185-8601, Japan*

(Received 8 September 2009; published 24 November 2009)

Scanning tunneling microscopy and density-functional theory have been combined to demonstrate structural transformations of steps of Si(100)-(2×1) induced by nondangling bond-terminated Cl adsorbates. We identify a stable, bridge-bonded step adsorption site and show that supersaturation facilitates the population of those sites, leading to rebonded atom etching, step retreat, and extensive terrace rearrangement from the diffusion of resultant atomic vacancy lines across the supersaturated surface. Similarities to H-Si(100) are briefly discussed.

DOI: [10.1103/PhysRevB.80.193307](https://doi.org/10.1103/PhysRevB.80.193307)

PACS number(s): 68.37.Ef, 61.72.Ff, 68.43.Fg

Steps play a critical role in epitaxial growth and, for this reason, the step structure of Si(100)-(2×1) has been extensively studied.<sup>1</sup> Two distinct step structures result from the symmetry of the diamond lattice. Single height  $S_A$  and double height  $D_A$  steps are parallel to the dimer rows of the upper terrace while  $S_B$  and  $D_B$  steps are perpendicular to them. Early calculations by Chadi<sup>2</sup> predicted two configurations for  $S_B$  and  $D_B$  steps: rebonded and nonrebonded. Figures 1(a) and 1(b) depict the (nonrebonded)  $n-S_B$  and (rebonded)  $r-S_B$  structures. Despite the incorporation of a highly strained bond, the  $r-S_B$  structure was predicted to be energetically favored, and scanning tunneling microscopy (STM) experiments showed that it dominates.<sup>3</sup> However, H-chemisorption alters the energy balance and the  $n-S_B$  structure dominates.<sup>4,5</sup>

Recent studies have sought to address the mechanism by which the step transforms from  $r-S_B$  to  $n-S_B$  upon adsorbate termination.<sup>6</sup> Theory has shown that dangling bonds (DBs) at nonrebonded steps are the least favored chemisorption sites for H,<sup>7</sup> and chemisorption should occur there only after all other DB sites are saturated at a coverage of 1 monolayer (ML). This has made studying step transformations difficult because it requires a controllable level of supersaturation to supply adsorbates to generate and saturate  $n-S_B$  DB's without inducing terrace etching.<sup>8</sup> The recent discovery of a mechanism that leads to Cl insertion into Si-Si surface bonds allows for such supersaturation,<sup>8</sup> offering a way to control chemisorption at steps.

We use STM and density-functional theory (DFT) to examine the evolution of the Si(100) step structure induced by Cl chemisorption at 700 and 725 K. We show that fine tuning of surface kinetic processes can direct inserted Cl atoms, Cl(i), from terraces to steps where they induce transformations on a manageable time scale. We identify a stable bridge-bonded adsorption site at the  $r-S_B$  step that promotes accumulation of Cl(i) and initiates the transformation process through a sequence of events that includes r-atom etching and step retreat. Significantly, this is accompanied by unexpected changes in the lower terrace. These results can be generalized because H atoms, which had been predicted to reside in precursor chemisorption sites,<sup>9–11</sup> can be the source of a similar restructuring process.<sup>12</sup>

The experiments were performed in ultrahigh vacuum (base pressure  $<5 \times 10^{-11}$  Torr) using an Omicron STM1

controlled by RHK SPM100 electronics. The Si wafers were  $p$  type, B doped to 0.01–0.02  $\Omega$  cm, and oriented within 0.5° of (100). Clean surface preparation has been described elsewhere.<sup>13</sup> Once the surfaces were demonstrated to be contamination free, they were reheated and exposed to  $Cl_2$  to achieve termination while still above room temperature, thereby minimizing water adsorption.<sup>13,14</sup>  $Cl_2$  was generated by an electrochemical cell of AgCl doped with 5 wt %  $CdCl_2$ , giving a  $Cl_2$  flux of  $1.67 \times 10^{-3}$  ML  $s^{-1}$ , where 1 ML =  $6.78 \times 10^{14}$   $cm^{-2}$ . Filled-state STM images were obtained at room temperature. The number of  $n-S_B$  and  $n-D_B$  step units and the extent of etching were determined by direct counting of 10–20 STM images,  $50 \times 50$   $nm^2$  in area, per datum point. The DFT calculations used the generalized gradient approximation<sup>15</sup> with plane-wave-based ultrasoft pseudopotentials<sup>16,17</sup> and an energy cutoff of 275.5 eV. The convergence criterion for geometry optimization was that all forces be less than  $5.14 \times 10^{-2}$  eV/Å. Slab models of five Si layers were used for Cl-terminated Si(100) with the dangling bonds of the bottom Si layer terminated with hydrogen.

Experiments have shown that exposure to atomic hydrogen below 625 K gives rise to  $n-S_B$  steps.<sup>4,12</sup> In contrast, there have been no reports of a similar change in step structure through Cl termination. The image in Fig. 1 shows the persistence of the  $r-S_B$  structure after a saturation exposure of  $Cl_2$  at 600 K. The bright dimer rows of the upper terrace terminate within the trough between dimer rows of the lower terrace. Rebonded Si atoms along the step have a circular appearance and can be easily distinguished from the oblong Si dimers. In Fig. 1, there is only one  $n-S_B$  unit. Significantly, our calculations indicate that the Cl-terminated  $n-S_B$  structure is favored by 1.8 eV/ $a$  over  $r-S_B$ , where  $a=3.84$  Å is the unit step length of Si(100). The rarity of the  $n-S_B$  structure indicates an insufficient concentration of Cl at the step to activate the transformation.

To investigate step transformations, we reasoned that supersaturating the terrace might lead to Cl(i) accumulation at the step. Accordingly, we exposed a saturated surface like that of Fig. 1 to  $Cl_2$  at 700 and 725 K. Under these conditions, single DBs are generated on the terrace by phonon-activated, electron-stimulated desorption of Cl atoms.<sup>18</sup> Once created, these now-active sites mediate the dissociative chemisorption of  $Cl_2$  with one atom terminating the DB and the other inserting into a Si-Si bond with a probability of

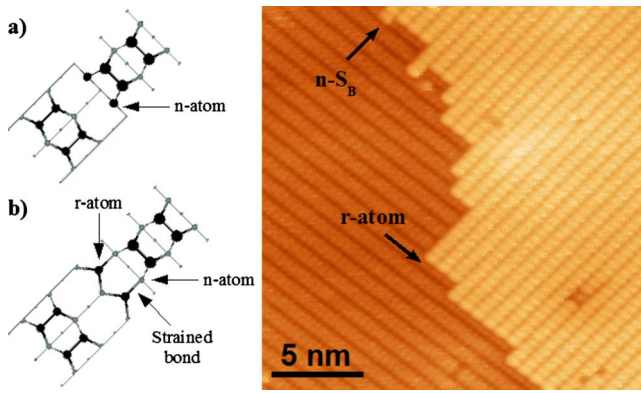


FIG. 1. (Color online) Models of (a)  $n\text{-S}_B$  and (b)  $r\text{-S}_B$  steps identifying r atoms and n atoms, which form a strained bond in (b). The filled-state STM image ( $-2.00$  V sample bias) shows an  $S_B$  step after saturation with Cl at 600 K. The step is predominantly  $r\text{-S}_B$ . r atoms appear circular and are adjacent to steps, whereas dimers have an oblong appearance.

$\sim 10\%$ .<sup>8</sup> Whereas insertion is expected at room temperature, it is difficult to quantify because Cl(i) is highly mobile and readily converts into Cl(a), an adsorbed Cl atom, at a DB.<sup>19,20</sup> Since the barrier for Cl(i)-Cl(a) decay is only  $\sim 0.15\text{--}0.3$  eV,<sup>21</sup> Cl(i) will decay before reaching the step. For saturated surfaces, this decay route is blocked.

Previous studies of Cl supersaturation above 750 K showed that Cl(i) atoms were lost when they paired on terrace dimers to form volatile  $\text{SiCl}_2$  units.<sup>8</sup> The activation barriers for Cl(i) diffusion<sup>22</sup> and pairing<sup>20</sup> are 0.3–0.4 and 2.5 eV, respectively. The large barrier to pair hinders etching and results in an increase in Cl(i) concentration with decreasing temperature, as demonstrated by Aldao *et al.*<sup>20</sup>

By reducing the temperature to 700–725 K, we have found a regime where diffusion is facile but pairing and terrace desorption of  $\text{SiCl}_2$  are minimal. Accordingly, mobile Cl(i) species can interrogate the surface and populate step sites. Instead of a relatively straightforward conversion of the step structure, however, we see that Cl(i) promotes etching of r atoms and, ultimately,  $n\text{-S}_B$  formation through the unexpected diffusion of vacancy lines across the saturated surface. This offers new insights into step dynamics while the diffusion of vacancy lines demonstrates that changes in the step structure can result in extensive restructuring of the lower terrace.

To establish an energetic correlation between Cl(i) accumulation and r-atom etching and  $n\text{-S}_B$  formation, we first determined a stable adsorption site for Cl(i) at the  $r\text{-S}_B$  step. Figure 2(a) depicts the initial Cl-terminated  $r\text{-S}_B$  step structure and Fig. 2(b) depicts that structure with Cl(i) forming a bridge bond between an r atom and an n atom. The total energy of Fig. 2(b) is 0.34 eV lower than that of Fig. 2(a).<sup>23</sup> Moreover, our calculations indicate that the step bridge-bonded Cl(i) is  $\sim 0.5$  eV lower in energy than terrace bound Cl(i) so that the site identified in Fig. 2(b) acts as a sink. Pairs of adjacent Cl(i)'s are bound with an energy of 0.4 eV.

Figures 2(c) and 2(d) depict a pathway whereby Cl(i) accumulation at bridge-bonded step sites creates a nonrebonded step. The structure of Fig. 2(c) was obtained by opti-

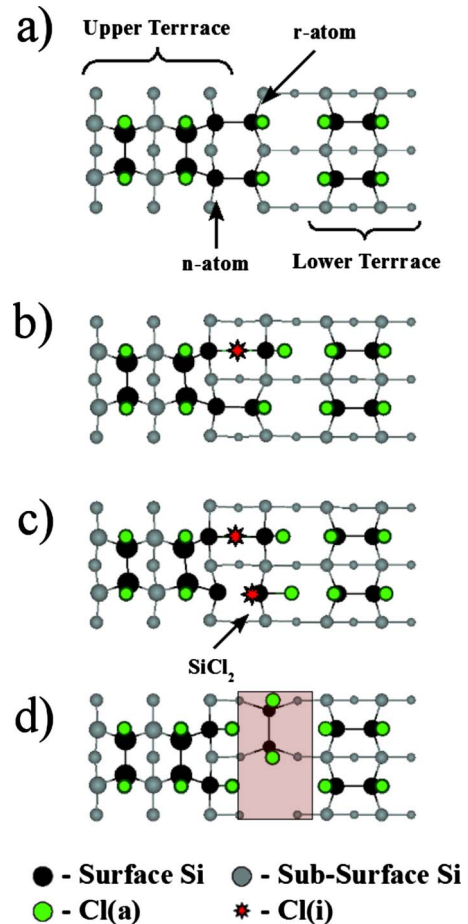


FIG. 2. (Color online) Calculated step structures relevant to r-atom etching. Periodic boundary conditions were applied to each calculation so that the top and bottom rows of Si atoms, as presented, are equivalent. Only the top three Si layers are shown. (a) Initial  $r\text{-S}_B$  step structure after Cl-termination. (b) Chemisorption of Cl(i) at the step forms a bridge-bond between an r atom and n atom. It is  $\sim 0.5$  eV lower in energy than for Cl(i) on the terrace. (c) Pairing of adjacent Cl(i)s produces volatile  $\text{SiCl}_2$  units, gaining 0.4 eV relative to two isolated units. (d) Desorption of both r atoms as  $\text{SiCl}_2$  gains 3.46 eV/a, relative to (a), with dimerization and Cl termination of the exposed Si layer. The box is one unit of an r-atom vacancy line.

mizing the geometry for two adjacent Cl(i) from two different initial conditions where both produced a bridge-bonded Cl(i) and a neighboring volatile  $\text{SiCl}_2$  with a DB at the step.  $\text{SiCl}_2$  desorption from both r-atom sites of a single step unit produces an atom-wide vacancy along an  $n\text{-D}_B$  step and gains 3.46 eV/a, assuming dimerization of the second layer Si atoms and Cl termination of the resulting DBs, as shown in Fig. 2(d).

The STM image in Fig. 3 was acquired after 8 h of continuous  $\text{Cl}_2$  exposure at 700 K. Atom-wide vacancy lines (AVLs), like that shown, were commonly observed along or close to  $S_B$  steps at 700 and 725 K. In contrast, they were never observed above 750 K because the delicate balance between Cl(i) accumulation at steps and  $\text{SiCl}_2$  desorption from terrace sites was disturbed in favor of terrace etching. From the relationship between kink length and step

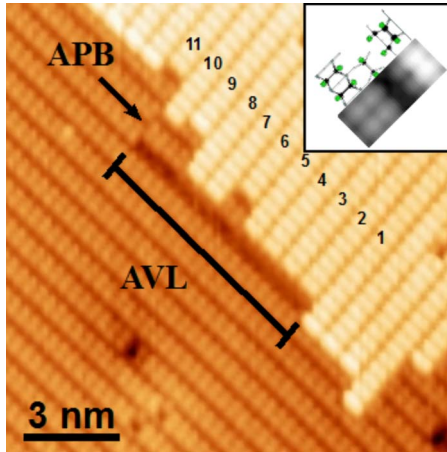


FIG. 3. (Color online) STM image ( $-2.00$  V) of an  $S_B$  step after 8 h of  $\text{Cl}_2$  exposure at 700 K. The AVL is composed of 18 r-atom vacancies. The units originating along step units 6, 9, and 10 have diffused to produce a continuous AVL and an APB where the dimers are out of registry with the lower terrace. Unit 9 has retreated by one dimer and regained the  $r\text{-}S_B$  structure despite undergoing r-atom etching. The inset is the calculated STM image ( $-2.00$  V) of the structure depicted in Fig. 2(d).

structure,<sup>24</sup> we can conclude that the AVL in Fig. 3 is derived from r-atom vacancies. The two-dimer-long kink separating step units 1 and 2 indicates that they should have the same structure. Unit 1 is  $r\text{-}S_B$  and unit 2 should be as well. Similarly, units 3–8 and 10 should be  $r\text{-}S_B$  while units 9 and 11 should be  $n\text{-}S_B$ . We conclude that the r atoms expected below these units have been etched. The calculated STM image of the structure in Fig. 2(d), shown in the inset, is in excellent agreement with experiment.

From Fig. 2(d), r-atom etching initially produces an  $n\text{-}D_B$  step because of the vacancy line along the step. This can convert to  $n\text{-}S_B$  if the vacancy line diffuses into the lower terrace while dimers shift toward the step. The antiphase boundary (APB) in Fig. 3 provides evidence of vacancy line diffusion because an APB is produced when dimers shift in half-dimer-length increments.<sup>25</sup> In Fig. 3, the dimers below step units 6, 9, and 10 are out of registry with the lower terrace and the AVL is one dimer length away from these units. As a result, units 6 and 10 resemble pristine unit 11, which is  $n\text{-}S_B$ . Unit 9 will be discussed below.

The rates of r-atom etching at 700 and 725 K were  $1.48 \pm 0.13 \times 10^{-4}$  and  $0.94 \pm 0.10 \times 10^{-4} a^{-1} \text{ min}^{-1}$ , respectively, whereas the rates of nonbonded step formation were  $2.17 \pm 0.29 \times 10^{-4}$  and  $0.66 \pm 0.31 \times 10^{-4} a^{-1} \text{ min}^{-1}$ . These rates were calculated from the r-atom vacancy concentration and the number of nonbonded step units ( $n\text{-}S_B$  and  $n\text{-}D_B$ ) per step length after 1, 2, 4, 8, 12, and 16 h of  $\text{Cl}_2$  exposure. Both display the inverse relationship with temperature seen for the concentration of  $\text{Cl}(i)$ .<sup>20</sup> Intriguingly, at 725 K the r-atom etch rate exceeds the nonbonded step formation rate. Since etching produces nonbonded steps, this suggests that some nonbonded step units have reverted back to the rebonded structure despite the substantial energy preference, 1.8 eV/a, for the former. In particular, the vacancies below step unit 9 of Fig. 3 indicate that etching has occurred even

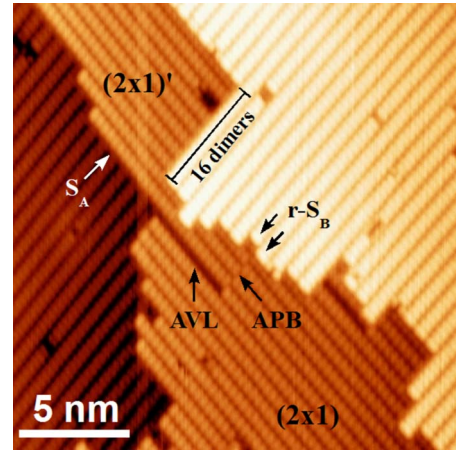


FIG. 4. (Color online) STM image ( $-2.25$  V) after 12 h of  $\text{Cl}_2$  exposure at 725 K. The  $(2 \times 1)$  and  $(2 \times 1)'$  domains reflect an extensive etching and terrace restructuring as each unit along the  $(2 \times 1)'$  domain has undergone r-atom etching and retreat. The resulting vacancy lines diffuse and annihilate at the  $S_A$  step. The AVL is a remnant that has yet to annihilate.

though r atoms can be seen along this step unit. In this case, the step unit must have retreated by a single dimer, through etching, and the  $n\text{-}S_B$  structure has reverted back to  $r\text{-}S_B$ .

Step retreat suggests a lower barrier for  $\text{Cl}(i)$  pairing on a step dimer than on a terrace dimer. De Wijs *et al.*<sup>22</sup> reported that the edge of a dimer vacancy accommodates  $\text{Cl}(i)$  and that the energy gained through  $2\text{SiCl}_2$  formation at the ends of such a vacancy is 0.3 eV greater than if it were to form in a defect-free region. They add that the desorption energy is  $\sim 0$  for the first and  $\sim 1.0$  eV for the second  $\text{SiCl}_2$  unit. By analogy, the  $S_B$  step should favor  $2\text{SiCl}_2$  formation as there is more room for bond distortion and relaxation. Accordingly,  $n\text{-}S_B$  and  $n\text{-}D_B$  step dimers will be sinks for  $\text{Cl}(i)$  after the structure depicted in Fig. 2(b) is eliminated during r-atom etching.  $\text{SiCl}_2$  desorption from these sites will cause the step to retreat by a single dimer and regain the  $r\text{-}S_B$  structure.

Figure 4 provides evidence that the processes discussed above occur on a much larger scale than was expected. The STM image was obtained after 12 h of continuous exposure at 725 K. Surprisingly, it shows a terrace with two major domains labeled  $(2 \times 1)$  and  $(2 \times 1)'$  that are shifted relative to one another by a half-dimer unit, as evidenced by the APB. As in Fig. 3, the AVL is indicative of r-atom etching while the APB can be associated with vacancy line diffusion away from the step. Since the step units bounded by the AVL all display the rebonded structure, each has retreated in a similar manner to unit 9 of Fig. 3, with further evidence given by the adjacent  $r\text{-}S_B$  units that are separated by a single-dimer-long kink across the APB.

Remarkably, the 16-dimer long kink identified in Fig. 4 signifies that etching and step retreat have occurred at each step unit along the  $(2 \times 1)'$  domain even though the AVL does not span the entire terrace below. We reason that the missing vacancy line segments have diffused across the terrace and annihilated at the  $S_A$  step. The AVL that can be seen is a remnant of this process and it has yet to annihilate at the step below. In this manner, the vacancy lines not only dif-

fused  $\sim 7$  nm away from the step, they also caused extensive terrace restructuring as the entire lower terrace shifted a half-dimer length (0.384 nm) toward the step in the wake of the diffusing vacancy lines. This implies a novel diffusion mechanism associated with vacancy lines, and it should rouse interest because conventional dimer vacancies cannot diffuse on Cl-saturated surfaces.<sup>26</sup>

These results have counterparts in the H-Si(100) system where the formation of  $n\text{-S}_B$  units has been associated with the creation of dihydride chains derived from the r-atom row.<sup>12</sup> In particular, the exposure conditions that produce dihydride chains ( $520 \leq T \leq 610$  K) coincide with an increased population of secondary, non-DB-terminated adsorption sites,<sup>11</sup> termed H(i) by analogy to Cl(i). These sites are similar to those predicted for Cl(i) (Ref. 22) and, likewise, H(i) is predicted to decay and diffuse with barriers of  $\sim 0.2$  (Ref. 27) and  $\sim 0.5$  eV,<sup>9</sup> respectively. Although the role of H(i) in dihydride chain formation has not been explicitly stated, it is presumed to be equivalent to that shown for Cl(i) in r-atom vacancy creation, namely, insertion, diffusion, ad-

sorption at step sites, and dihydride formation. Furthermore, H(i) was shown to facilitate dihydride chain diffusion onto the terrace,<sup>12</sup> whereas a similar diffusion mechanism for r-atom vacancies would not be possible since energetics dictate  $\text{SiCl}_2$  desorption as opposed to  $\text{SiCl}_2$  diffusion.

The similarities of r-atom vacancies and dihydride chains are suggestive of a general interaction of monatomic adsorbates with  $\text{S}_B$  steps when the adsorbate coverage exceeds 1 ML. As shown here, the r-atom bridge-bonded adsorption site of Fig. 2(b) accommodates the excess adsorbates and, in turn, they alter the step energetics leading to step transformations. These results further highlight the necessity to incorporate these so-called inserted adsorbates in descriptions of most surface processes as the coverage nears, and exceeds, 1 ML.

We thank K.S. Nakayama for useful discussions. The DFT calculations were performed with the Tokyo *ab initio* program package.

- 
- <sup>1</sup>S. Wolf and R. N. Tauber, *Silicon Processing for the VLSI Era* (Lattice, Sunset Beach, California, 1986).
- <sup>2</sup>D. J. Chadi, Phys. Rev. Lett. **59**, 1691 (1987).
- <sup>3</sup>R. J. Hamers, R. M. Tromp, and J. E. Demuth, Phys. Rev. B **34**, 5343 (1986).
- <sup>4</sup>A. Laracuente and L. J. Whitman, Surf. Sci. **476**, L247 (2001).
- <sup>5</sup>S. Jeong and A. Oshiyama, Phys. Rev. Lett. **81**, 5366 (1998).
- <sup>6</sup>A. R. Laracuente and L. J. Whitman, Surf. Sci. **545**, 70 (2003).
- <sup>7</sup>E. Pehlke and P. Kratzer, Phys. Rev. B **59**, 2790 (1999).
- <sup>8</sup>A. Agrawal, R. E. Butera, and J. H. Weaver, Phys. Rev. Lett. **98**, 136104 (2007).
- <sup>9</sup>E. S. Tok, J. R. Engstrom, and H. Chuan Kang, J. Chem. Phys. **118**, 3294 (2003).
- <sup>10</sup>W. Widdra, S. I. Yi, R. Maboudian, G. A. D. Briggs, and W. H. Weinberg, Phys. Rev. Lett. **74**, 2074 (1995).
- <sup>11</sup>A. Kutana, B. Makarenko, and J. W. Rabalais, J. Chem. Phys. **119**, 11906 (2003).
- <sup>12</sup>Y. Suwa, M. Fujimori, S. Heike, Y. Terada, Y. Yoshimoto, K. Akagi, O. Sugino, and T. Hashizume, Phys. Rev. B **74**, 205308 (2006).
- <sup>13</sup>B. R. Trenhaile, A. Agrawal, and J. H. Weaver, Appl. Phys. Lett. **89**, 151917 (2006).
- <sup>14</sup>S. Y. Yu, H. Kim, and J. Y. Koo, Phys. Rev. Lett. **100**, 036107 (2008).
- <sup>15</sup>J. P. Perdew, K. Burke, and Y. Wang, Phys. Rev. B **54**, 16533 (1996).
- <sup>16</sup>D. Vanderbilt, Phys. Rev. B **41**, 7892 (1990).
- <sup>17</sup>K. Laasonen, A. Pasquarello, R. Car, C. Lee, and D. Vanderbilt, Phys. Rev. B **47**, 10142 (1993).
- <sup>18</sup>B. R. Trenhaile, V. N. Antonov, G. J. Xu, A. Agrawal, A. W. Signor, R. E. Butera, K. S. Nakayama, and J. H. Weaver, Phys. Rev. B **73**, 125318 (2006).
- <sup>19</sup>Q. Gao, C. C. Cheng, P. J. Chen, W. J. Choyke, and J. T. Yates, Jr., J. Chem. Phys. **98**, 8308 (1993).
- <sup>20</sup>C. M. Aldao, Abhishek Agrawal, R. E. Butera, and J. H. Weaver, Phys. Rev. B **79**, 125303 (2009).
- <sup>21</sup>G. A. de Wijs and A. Selloni, Phys. Rev. Lett. **77**, 881 (1996).
- <sup>22</sup>G. A. de Wijs, A. De Vita, and A. Selloni, Phys. Rev. B **57**, 10021 (1998).
- <sup>23</sup>The energy contribution of full and half  $\text{Cl}_2$  molecules and  $\text{SiCl}_2$  units were used to ensure a consistent number of Cl and Si atoms throughout the calculations to allow for comparison.
- <sup>24</sup>H. J. W. Zandvliet, Rev. Mod. Phys. **72**, 593 (2000).
- <sup>25</sup>C. F. Herrmann, D. Chen, and J. J. Boland, Phys. Rev. Lett. **89**, 096102 (2002).
- <sup>26</sup>G. J. Xu, E. Graugnard, V. Petrova, K. S. Nakayama, and J. H. Weaver, Phys. Rev. B **67**, 125320 (2003).
- <sup>27</sup>E. S. Tok and H. C. Kang, J. Chem. Phys. **115**, 6550 (2001).